eprints@whiterose.ac.uk
https://eprints.whiterose.ac.uk/

Wear

Chip formation and wear mechanisms of SiAlON and whisker-reinforced ceramics when turning Inconel 718.
--Manuscript Draft--

Manuscript Number:	WEA-D-21-00369R2
Article Type:	Full length article
Keywords:	SiAlON; Whisker-reinforced Alumina; Machining Inconel 718; Turning; chip morphology; Ceramic Cutting tools
Corresponding Author:	Tom Slatter The University of Sheffield Sheffield, United Kingdom
First Author:	Luke Osmond, BSc
Order of Authors:	Luke Osmond, BSc
	David Curtis, PhD
	Tom Slatter
Abstract:	Inconel 718 has found use in many demanding applications due to its high temperature fatigue strength, hardness and low thermal conductivity. These material properties present a challenge to productive and high quality (surface finish) machining and promote rapid tool wear. The work presented here describes the chip formation and wear mechanisms of silicon nitride (Si_3N_4) based ceramic SiAlON and silicon carbide whiskers reinforced alumina (WRA) ($Al_2O_3 + SiC_w$) round (RNGN) inserts, when turning solution-annealed Inconel 718 (27<HRC<30) with a 10% concentration cutting fluid. Four sets of cutting trials were conducted at a cutting speed of 250m/min and another four at 300m/min. The results show that using SiAlON turning inserts at a cutting speed of 300m/min delivered the best results in terms of tool flank wear, total tool life, and work-piece surface finish. The morphology of the Inconel 718 chip, at cutting speeds above 250m/min, presents an intense shear band localisation in the primary shear zone of the chip/tool interface, which leads to chip segmentation.
Suggested Reviewers:	Stephen Veldhuis McMaster University veldhu@mcmaster.ca
	Roberto Polvorosa Universidad del Pais Vasco roberto.polvorosa@ehu.eus
	Knut Sørby Norwegian University of Science and Technology Faculty of Engineering Science and Technology: Norges teknisk-naturvitenskapelige universitet Fakultet for ingeniorvitenskap knut.sorby@ntnu.no

Chip formation and wear mechanisms of SiAlON and whisker-reinforced ceramics when turning Inconel 718.

Luke Osmond[1, 3], David Curtis[2], Tom Slatter[3]

[1]Industrial Doctorate Centre in Machining Science, Advanced Manufacturing Research Centre, The University of Sheffield, Catcliffe, Rotherham, U.K. S60 5TZ

[2]Advanced Manufacturing Research Centre, The University of Sheffield, Advanced Manufacturing Park, Catcliffe, Rotherham, U.K. S60 5TZ

[3]Department of Mechanical Engineering, The University of Sheffield, Mappin Street, Sheffield, U.K. S1 3JD

Abstract

Inconel 718 has found use in many demanding applications due to its high temperature fatigue strength, hardness and low thermal conductivity. These material properties present a challenge to productive and high quality (surface finish) machining and promote rapid tool wear. The work presented here describes the chip formation and wear mechanisms of silicon nitride (Si_3N_4) based ceramic SiAlON and silicon carbide whiskers reinforced alumina (WRA) ($Al_2O_3 + SiC_w$) round (RNGN) inserts, when turning solution-annealed Inconel 718 (27<HRC<30) with a 10% concentration cutting fluid. Four sets of cutting trials were conducted at a cutting speed of 250m/min and another four at 300m/min. The results show that using SiAlON turning inserts at a cutting speed of 300m/min delivered the best results in terms of tool flank wear, total tool life, and work-piece surface finish. The morphology of the Inconel 718 chip, at cutting speeds above 250m/min, presents an intense shear band localisation in the primary shear zone of the chip/tool interface, which leads to chip segmentation.

Keywords: SiAlON, Whisker-reinforced Alumina, Machining Inconel 718, Turning, Chip Morphology, Ceramic Cutting tools

1 Introduction

Nickel-based super alloy, Inconel 718, is one of the most widely utilised materials of its type in industry and is commonly used in the manufacture of aerospace components such as bladed disks (blisks), turbine and compressor discs, and compressor aerofoils. It is also used to manufacture oil and gas components such as well-heads and Christmas tree valves. The austenitic face-centre, cubic crystal structure of Inconel 718 contains a fine dispersion of gamma prime (γ') intermetallic compound Ni_3 (Al, Ti) in a matrix of nickel solution which contains chromium, iron, niobium and molybdenum, resulting in a high strength microstructure [1-3]. The microstructure exhibits very high temperature strength and creep

resistance, and work hardens rapidly during the machining process [4-7]. Even when solution-annealed, the Inconel 718 microstructure still creates a very challenging machining environment for cutting tools. Cutting tool materials therefore require high wear resistance, high hot hardness and good chemical stability at cutting temperatures of over 1000°C.

Ceramic cutting tools can be utilised to reduce the cost of machining nickel-based alloys by means of increasing productivity through exploitation of the metal removal rates (MRR) achievable by using ceramic turning inserts at the correct cutting speeds, feed rates and depths of cut. There is a trade off with using ceramic turning inserts, as higher metal removal rates also increase the amount of wear, reduce the tool life and increase the number of tool changes that are necessary during a roughing or semi roughing turning operation. These factors should be taken into account when utilising ceramic turning inserts for component manufacture. Increasing productivity comes as result of further understanding of the wear mechanisms which affect SiAlON and whisker-reinforced alumina ceramic turning (RNGN) inserts when employing the appropriate (or not) use of coolant [8, 9]. High pressure (<10MPa) cutting fluid has shown to have a positive effect on the tool life of ceramic turning inserts and has proven to be beneficial in reducing the wear mechanisms which break down the tool [10]. In continuous ceramic turning operations, the temperature on the rake face of the insert can reach 1200°C; these high cutting temperatures quickly influence the degradation of the SiAlON or WFA ceramic turning insert via diffusion wear mechanisms, resulting in the creation of wear craters on the rake face, which quickly become susceptible to notch wear.

Heavy use of water-soluble metal working fluids when machining difficult to machine alloys, has been proven to enhance the cutting performance of carbide cutting tools, reduce the effects of wear and significantly reduce the amount of heat in the shear zone between the cutting tool and workpiece. The coolant serves as a way of extracting some of the heat away from the shear zone interface between the Inconel 718 workpiece and the ceramic turning insert and dilute the effects of diffusion wear. Previous studies [11,12] established that high pressure cooling strategies help to create a hydraulic wedge between the tungsten carbide cutting tool and the Inconel 718 workpiece. When ceramic turning inserts are utilised however, the coolant fails to wedge in between the work-piece material and the cutting edge of the tool, prevented by a gas bubble in the cutting zone, formed when the fluid vaporises because of the high seizure conditions in the tool-chip interface when it comes into contact with the tool edge. This also contributes to tool wear because of the acceleration of abrasive particles into the face of the cutting tool. The use of high-pressure coolant helps to promote improved chip-breaking characteristics but also leads to the accelerated notch wear of the

ceramic turning insert. Other studies [13 -15] have also focused on understanding the impact of cryogenic, minimum quantity lubrication (MQL) and solid MQL on the depth of microhardness and induced residual stresses when machining Inconel 718 with whisker-reinforced alumina (WRA) (Al_2O_3 + SiC_w) ceramic cutting tools. These studies concluded that cryogenic cooling help to reduce residual stresses in the surface of the Inconel 718, and the application of solid MQL allows for a better surface finish to be attained at high cutting speeds of 350m/min. Another MQL focused study [16] has used ceramic turning tools in an MQL environment, which has resulted in significant reductions in tool wear and attained better surface finishes when compared to turning hardened EN31 steel under dry cutting conditions.

Inconel 718, as is typical of this class of material, will produce a serrated chip morphology. These saw-tooth like chips are produced during the cutting process due to the formation of cyclic cracks at the free surface of the chip [17].

This type of material behaviour is particularly exhibited by Inconel 718 when it is machined at high speed. When whisker-reinforced alumina (WRA) (Al_2O_3 + SiC_w) ceramic cutting tools are used, there are variable wear mechanisms which manifest along the tool–chip interface that are ultimately attributed to the deviations in plastic deformation energy that the inserts experience during the turning process [18]. The complex deformation of Inconel 718 chips above cutting speeds of 60m/min generates a principally inhomogeneous chip and the tool generates diverse stress states during the chip formation process, which thus form the segmented serrated sections of the chip [19-20].

The main challenge that becomes apparent when turning Inconel 718 with ceramic turning inserts is that high rates of wear are evident if the cutting parameter are not selected correctly. The cutting forces which are experienced by the ceramic cutting inserts are directly related to the cutting speed, cutting edge geometry, depth of cut and feed rate. The selection of Inconel 718 material grades and specifications is very much component specific. This particular study focuses on turning solution annealed Inconel 718. The main motivation for this research therefore is the need to understand and characterise the effects of turning solution-annealed Inconel 718. Solution annealed Inconel 718 was selected for this study as this particular alloy specification is extensively machined in rough and semi rough machining operations in the aerospace sector and in the oil and gas sector. Once the rough and semi rough machining operations are completed the components are age hardened and finish machined. The work presented here was conducted at two different cutting speeds, with chamfered and non-chamfered ceramic turning inserts and with a constant depth of cut and feed rate.

3

2   Materials and Methods

2.1   Machine Tool

A high precision turning machining centre (a DMG MORI NLX2500/700), fitted with a high-pressure coolant delivery system, this was used throughout this work. A refractometer was used throughout the machining trial experiments to take measurements of the cutting fluid (Blaser-Swisslube Vasco 7000 water-miscible, vegetable ester based, high performance cutting fluid). The cutting fluid concentration level was monitored and maintained at 10%. Flood cutting fluid supply was used in all the eight sets of test cuts and kept at 2 MPa pressure.

2.2   Work-piece material

A single workpiece piece of solution-annealed (27HRC) Inconel 718 round bar, nominally 100mm diameter and 350mm in length, was used throughout this work. The chemical composition and mechanical properties of Inconel 718 (AMS5662) are given in Table 1 and Table 2.

Table 1. Chemical composition of Inconel 718 (AMS5662) (%) [21]

C	Mn	Si	P	S	Cr	Ni	Co	Mo	Nb+Ta	Ti
0.040	0.08	0.08	<0.015	0.002	18.37	53.37	0.23	3.04	5.34	0.98
Al	**B**	**Ta**	**Cu**	**Fe**	**Ca**	**Mg**	**Pb**	**Bi**	**Se**	**Nb**
0.50	0.004	0.005	0.04	17.80	<0.010	<0.010	0.0001	0.00001	<0.0001	5.33

Table 2. Mechanical Properties of Inconel 718 (AMS5662) [21]

Yield stress (MPa)	Tensile stress (MPa)	Strain (%)	Elastic modulus (GPa)	Thermal conductivity (W/m K)	Density (kg/m³)
751	939	23.3	206	11.6	8470

2.3   Cutting tools

Two different SiAlON ceramic turning inserts tools were used during the machining trial and they were held in the machining centre by the supplier-recommended tool holder (a CRGNL 2525 M12-07). The two grades of ceramic that were used in the machining trial have slightly different material characteristics. The typical properties of whisker-reinforced alumina (Al_2O_3

4

+ Si C_w) ceramic inserts and silicon nitride (Si_3N_4) based ceramics (SiAlON) inserts can be viewed in Table 3. G. Brandt et al [22] discuss in their research the route of manufacture of whisker-reinforced alumina inserts. The hot-pressing process generates a high strength anisotropic whisker distribution of silicon carbide, which is preferably perpendicular to the face of the insert. The SiAlON inserts are a mixture of silicon nitride, aluminium oxides and yttrium oxide. The typical percentage of elements that are present in whisker-reinforced alumina and SiAlON ceramic inserts is shown in Table 3.

Table 3. Ceramic and carbide Inserts material properties. [23] [6]

Material properties	Whisker-reinforced alumina	SiAlON
Typical Tool composition.	75% Al_2O_3, 25% SiC	77% Si_3N_4 + 13% Al_2O_3 + 10% Y_2O_3
Grain size (μm)	Not Available	1
Density (g cm^{-3})	3.7	3.2
Hardness (HV) at 20°C	2000	1700
Hardness (HV) at 800°C	Not Available	850-1350
Fracture toughness (MNm$^{-3/2}$)	8	6
Young's modulus (kN mm^{-2})	390	300
Thermal conductivity (w m^{-1} °C)	32	23
Coefficient of thermal expansion (x10^{-6}–°C)	8.0	3.2

The tooling assembly is shown in Figure 1A and had to be removed repeatedly throughout the machining trial so that the ceramic inserts could be analysed, and a wear measurement could be taken. A simple nut and bolt arrangement was utilised as an end stop, so that the ceramic tool assembly could easily be replaced in the machine in the same position, and this is shown in Figure 1B. The outlet of the high-pressure coolant system was positioned in the conventional manner.
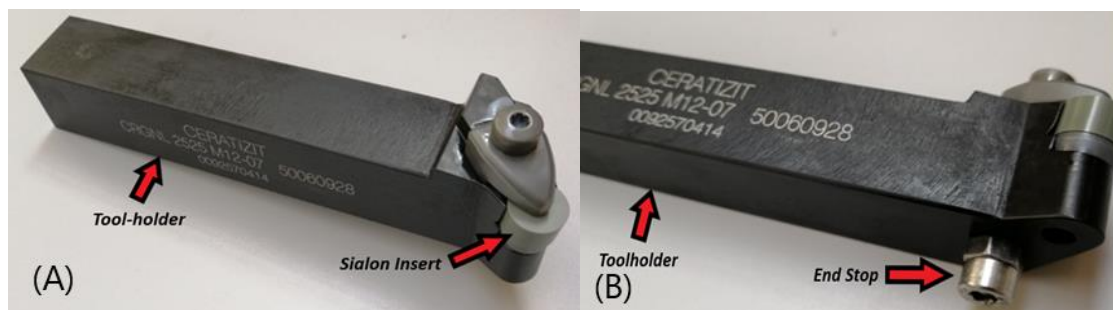

Figure 1. Tool-holder assembly with SiAlON insert installed (A). Tool-holder assembly with location end stop visible on the underside (B).

2.4 Experimental procedure

The workpiece was held in bored-out soft jaws and supported at the other end with a driven high rigidity tailstock with a revolving centre. During the experimental trials, the cutting conditions shown in Table 4 were employed. The cutting parameters for each insert were as stipulated by a previous study [5] to enable comparison. Each combination of tool material and process parameters was tested twice, as can be seen in Table 4. Test cut numbers 1.1 - 1.2, 2.1-2.2, 3.1-3.2 and 4.1-4.2 were conducted at 250m/min, with a feed rate of 0.20mm/rev and constant depth of cut (DoC) of 2.0mm. Test numbers 5.1-5.2, 6.1-6.2, 7.1-7.2 and 8.1-8.2 were conducted at 300m/min, with a feed rate of 0.20mm/rev and constant depth of cut (DoC) of 2.0mm.

The total volume of material removed by each insert in each test was 273 cm^3. As the turned diameter reduced, the length of the cut had to be increased to attain the same volume of material removal. The turning speeds (revolutions per minute) were increased for each stage, as the bar diameter was reduced, to keep the cutting velocity consistent at 250m/min for the first set of tests and at 300m/min for the second set of tests. The length of each pass was also slightly different to ensure a safe exit of each cut was achieved and that the inserts were not shocked. Every test cut was rolled in to cut to avoid shocking the insert. This is to reduce the effect of driven wear mechanisms on initial entry into cut.

Table 4. Cutting conditions for each test.

Test Cut number	Tool material	Insert Identification Letter	Cutting Speed (m/min)	Feed Rate (mm/rev)	Depth of Cut (mm)	Material Removal Rate (mm^3/s)
1.1, 1.2	SiAlON Grade 1	A	250	0.20	2	160
2.1, 2.2	SiAlON Grade 1 (chamfered)	B	250	0.20	2	160
3.1, 3.2	SiAlON Grade 2	C	250	0.20	2	160
4.1, 4.2	Whisker - Reinforced Alumina	D	250	0.20	2	160
5.1, 5.2	SiAlON Grade 1	A	300	0.20	2	200
6.1, 6.2	SiAlON Grade 1 (chamfered)	B	300	0.20	2	200
7.1, 7.2	SiAlON Grade 2	C	300	0.20	2	200
8.1, 8.2	Whisker – Reinforced Alumina	D	300	0.20	2	200

2.5 Tool wear monitoring

Images of the new, unused inserts were taken for reference before machining took place. Inspection of the inserts was performed twice further: firstly, after two-thirds of the volume of material was removed and secondly, when all the volume of material was removed. Frequent examination of the ceramic inserts was necessary to assess if there was any wear on the cutting edge and to create a before-cut, during-cut and after-cut image profile for each insert. This information allowed for assessment of the wear that had been generated during each machining trial. Once the level of flank wear had exceeded the default wear scar limit of 1mm, the test cut was stopped and classified as a failure.

2.6 Chip Preparation

Swarf (serrated chips removed from the material during machining) were collected during the machining trial. The four chip samples were then mounted separately in electrically conductive material (Bakelite) for use in electron microscopy techniques, which is shown in Figure 2.
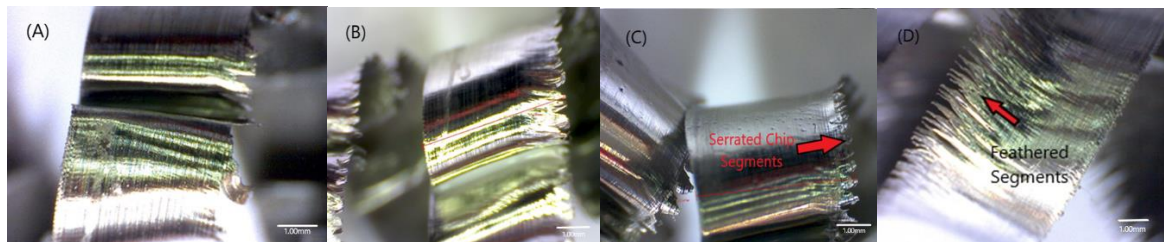

Figure 2 - Swarf produced by; insert D (Test 4.2) (Vc = 250m/min, F = 0.20mm/rev, Depth of Cut = 2mm) (A), insert C (Test 3.1) (Vc = 250m/min, F = 0.20mm/rev, Depth of Cut = 2mm) (B), insert D (Test 8.1) (Vc = 300m/min, F = 0.20mm/rev, Depth of Cut = 2mm) (C), insert C (Test 7.2) (Vc = 300/min, F = 0.20mm/rev, Depth of Cut = 2mm) (D).

The mounted samples were prepared via grinding and polishing operations using Carbi-met 320 [P400] 35 µm grit size pad, Carbi-met 400 [P800] 22 µm grit size pad and Carbi-met 600 [P1200] 15 µm grit size pad.

3 Results

3.1 Tool wear (250m/min tests)

The first set of test cuts involved using insert A (SiAlON grade 1, 250m/min, 0.20 mm/rev, 2mm DoC). Large vibrations were encountered over 50 % of the first cut due to the faster than expected degradation of the cutting edge.

Figures 3 shows the wear scar of insert A after the first ceramic cut that was conducted on the Inconel 718 round bar. The tool was subsequently failed because the wear scar that was generated in the first cut exceeded the default wear scar limit of 1mm.
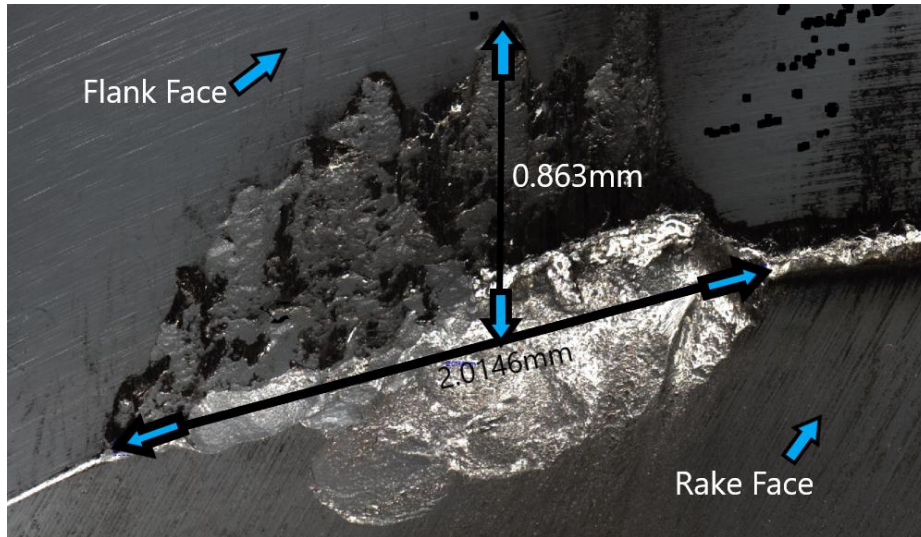
Figure 3. Image of the width and height of the wear scar on insert A (SiAlON grade 1). Image captured on Alicona infinite-focus SL microscope.

Figure 4 clearly shows the wear scar that was generated after the first cut. The images show the flank edge of the insert at the top part of image and rake face on the bottom part of the image. The large crater that is visible clearly shows signs of flank wear on the top part of the image and crater wear and notch wear. Thermal cracks are also visible going from the middle of the image all the way out to the far right of the image.
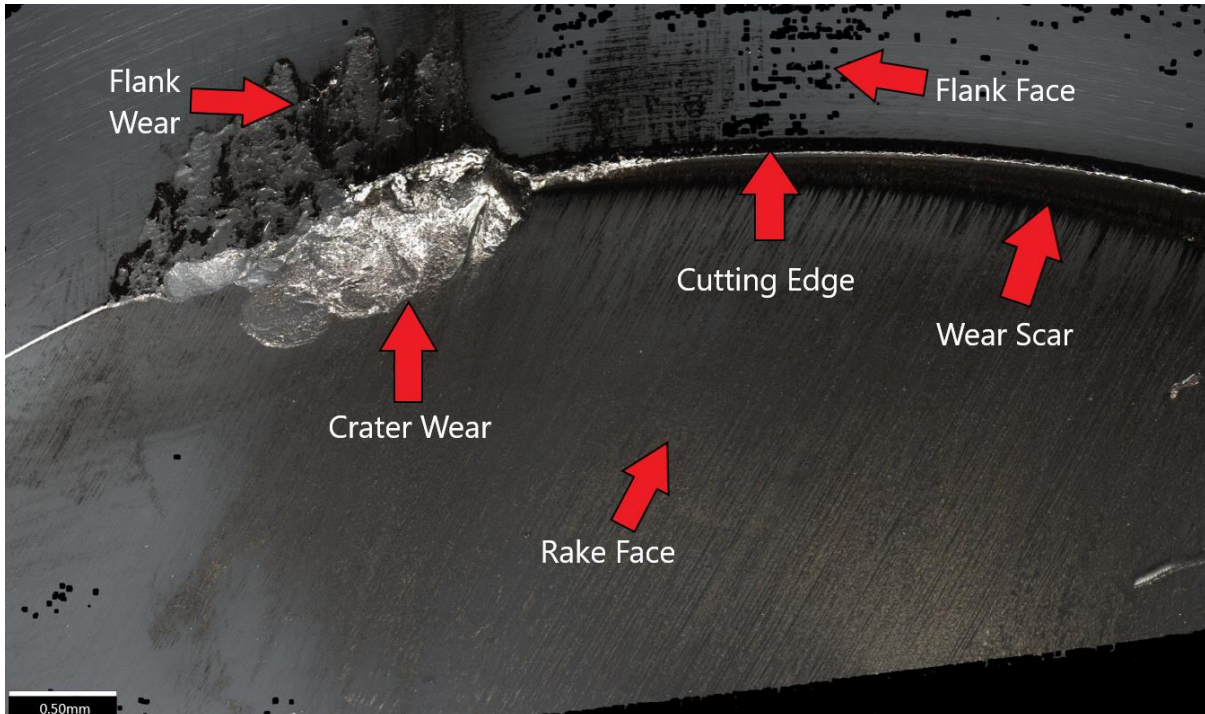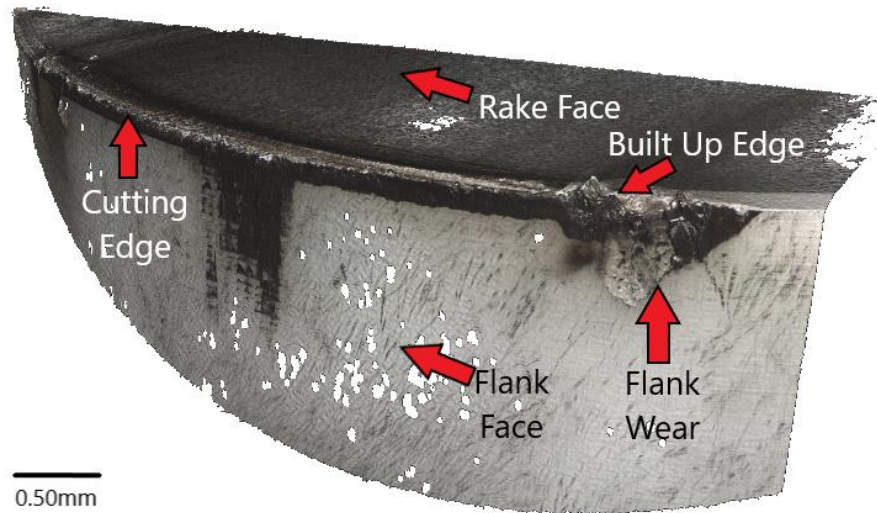

Figure 4. Wear scar on turning insert B (SiAlON grade 1) after test cut 1.1. Test was classed as a failure.

A second test utilised insert B (SiAlON grade 1), but with a 0.1mm chamfer on at the same cutting conditions. Vibrations were encountered again, over 25 % of the second cut, but at a

reduced level, apparently due to the chamfer. Figure 5 has managed to capture the entire wear scar. The potential reason for large amounts of the wear is likely due to the high fluctuation of specific cutting forces that were being generated in the shear zone between the work-piece and the insert. The fluctuations in these specific forces created a segmented chip.

Figure 5. Wear scar on turning insert B (SiAlON grade 1) after test cut 2.2,

The third set of test cuts of the machining trial used insert C (SiAlON grade 2). Figure 6 shows a wear scar on turning insert C (SiAlON grade 2) after test cut 3.2.
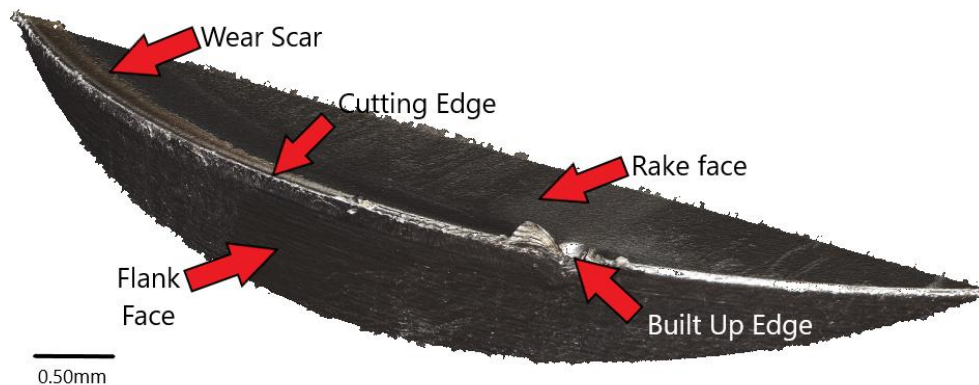
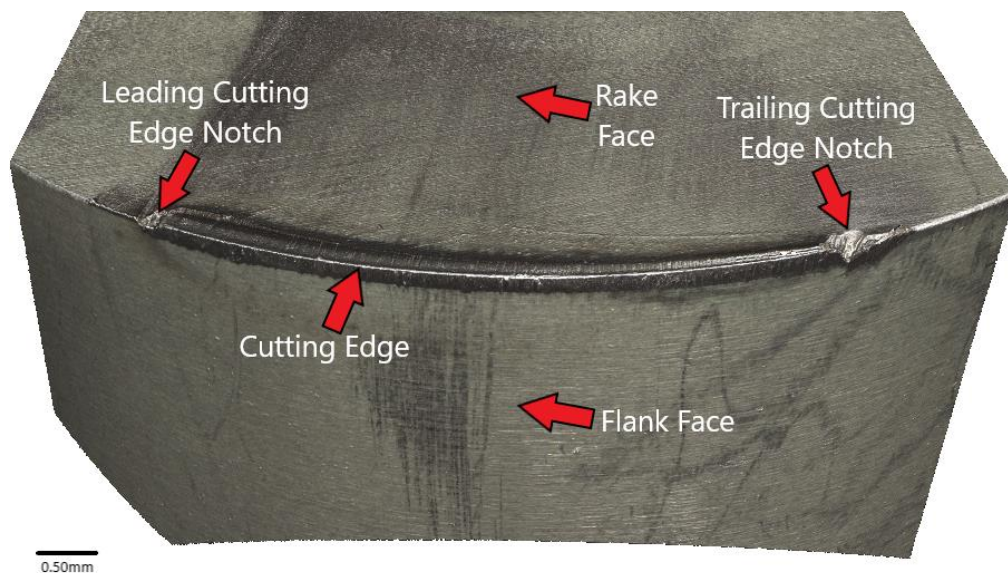Figure 6. Wear scar on turning insert C (SiAlON grade 2) after test cut 3.2.

Tool 5 provided noticeable results when compared to first two sets of test cuts with the insert demonstrating excellent resistance to abrasion. Insert C showed no real signs of flank wear, crater wear or notch wear. The cutting edge was in very good shape after the first test cut. There were slight signs of abrasion on the rake face but that was to be expected considering the cutting conditions. Insert C is a standard grade for machining nickel-based alloys and it performed as expected.

The same flank wear and notch wear patterns that can be seen with insert A and insert B also affect insert C, but visually show less abrasive wear of the rake and flank face of the insert. The reason for the improved resistance to abrasion, flank wear and notching are that that insert C seems to demonstrate higher hot hardness and a tougher microstructure. The tougher microstructure will come from the inclusion of more β-SiAlON grains, and the abrasion resistance and hot hardness will come from the α-SiAlON. The β-SiAlON is a solid solution of aluminium and oxygen in beta Si_3N_4, and α-SiAlONs are a solid solution of yttrium, oxygen and nitrogen in alpha Yx (Si Al)12 (O N)16. From the visual information captured in Figure 6, the α- and β- SiAlONs in insert C look to have been hot-pressed to form an insert with superior hot hardness, toughness and abrasion resistance when compared to insert A and insert B.

The fourth test of the machining trial used insert D (whisker-reinforced alumina). The test consisted of two cuts at equal length and depth. In Figure 7, a wear scar on turning insert D after test cut 4.2 is shown. During the fourth test, very few vibrations were encountered over of the course of the fourth cut. The reason for the little vibration is likely due to the high strength and abrasion resistance of the cutting edge. The mechanical properties of whisker-reinforced alumina inserts are shown in Table 4, indicating that whisker-reinforced alumina grades of insert have a higher modulus and fracture toughness when compared to insert A and B, which aids the inserts' ability to resist the intense cutting conditions.


Figure 7. Wear scar on turning insert D (whisker-reinforced alumina) after test cut 4.2.

The fourth set of test cuts provided noticeable results when compared to first two sets of test cuts. Insert D again showed no real signs of flank wear, crater wear or notch wear. The cutting edge was in very good shape after test cut 4.1. There were signs of abrasion on the

rake face, which are caused by high temperatures being generated in the tool/chip interface. The high temperatures are due to the low thermal conductivity of Inconel 718 and the abrasion of the cutting tool against hard Ni_3Nb particulates distributed within the Inconel 718 material. The lack of wear is visible in Figures 7 and the insert delivered as expected.

Insert D suffered from similar flank, rake and notch wear patterns that can be seen with inserts A, B and C but were significantly less than insert A and B. The reasons for the high abrasion resistance is due to the higher overall hardness of alumina than that of silicon nitride (Si_3N_4) based ceramics such as SiAlON. The rake face wear of insert D is slightly worse than that of insert C. From the information in Figure 8, it appears that whisker-reinforced alumina inserts have lower hot hardness than that of that SiAlON.
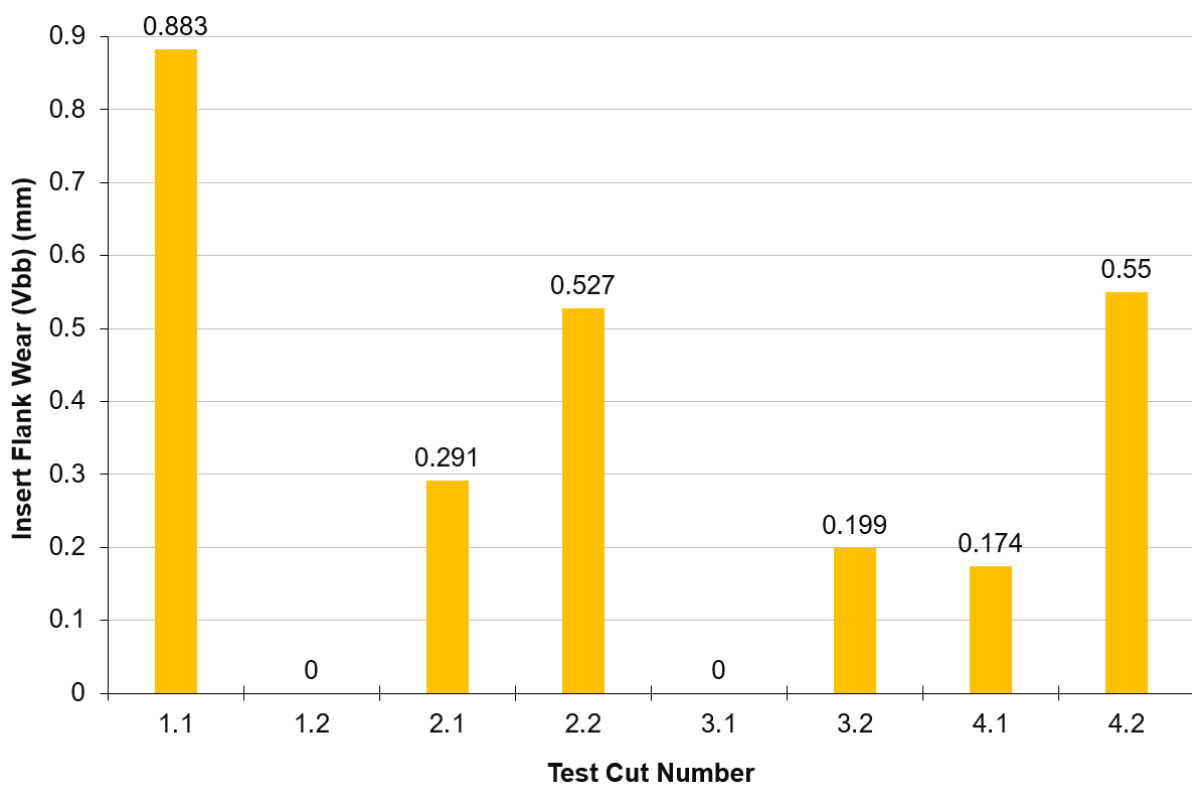
Figure 8. Measured flank wear (Vbb) experienced for each test cut at a cutting speed of 250m/min.

However, the silicon carbide whiskers distributed throughout the alumina matrix provide increased fracture resistance and abrasion resistance. The abrasion resistance of insert C was better than insert A and B and highlights that insert C has marginally better wear resistance than insert D. Each test cut was repeated twice so that correct amount of material was removed. Figure 8 represents raw data directly gathered from the machining trial, so no error bars have been included in the graph.

3.2 Tool Wear (300m/min tests)

During the fifth set of test cuts (SiAlON insert A, 300m/min, 0.20 mm/rev, 2mm DoC), there were no signs of any large vibrations as encountered in the first test.

Figure 9 show the wear scar on turning insert A after test cut 5.2. The reason for the reduction in vibration is likely due to the higher surface speed and the lack of degradation is clearly visible. The increase in surface speeds has generated higher cutting temperatures in the primary and secondary deformation zones, which in turn reduces cutting forces required to cut the material. The higher surface speed also reduces the ploughing effect that caused the earlier vibration with insert A and insert B in test cuts 1.1 and 2.1.
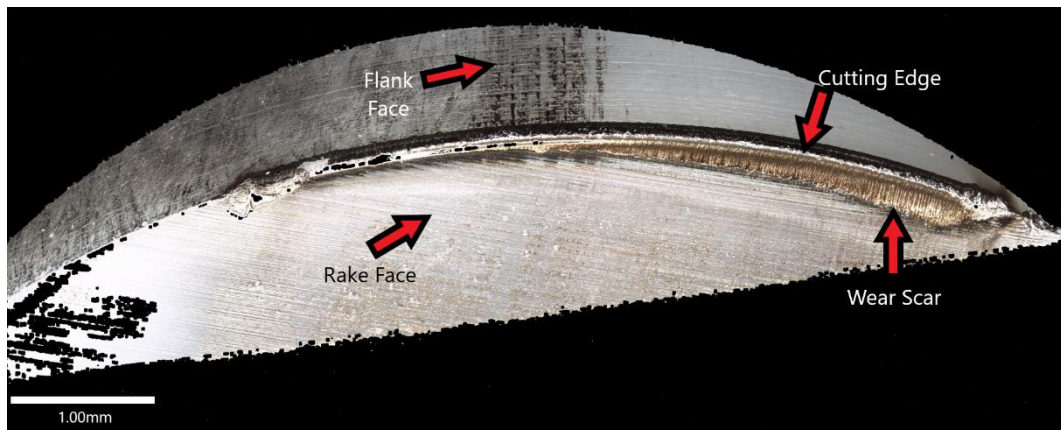

Figure 9. Wear scar on turning insert A (SiAlON grade 1) after test cut 5.2.

Figure 9 highlights the improvement in wear resistance. The improvements in wear resistance have come from an increase in surface speed from 250m/min to 300m/min, which has definitely had a positive effect and helped reduced the amount of wear that is generated whilst in cut. The higher surface speed has managed to stabilise the cutting process and helped to reduce the vibration that was experienced with insert A in test cut 1.1. The increase in surface speed will have increased the cutting temperature between the Inconel 718 workpiece and the insert, hence this reduces the yield point of the Inconel 718 and the subsequent cutting forces that the insert A experiences. The rake face wear that is visible in Figure 9 indicates better abrasion resistance, which is down to localised heating and softening of the Inconel 718, in turn reducing the amount of wear deformation that the cutting insert experienced.

The sixth set of test cuts used insert B (SiAlON grade 1). Again, the test consisted of two cuts at equal length and depth. Figure 10 shows a wear scar on turning insert B after test cut 6.2. The 0.10mm chamfer on insert B together with the increase in surface speed, delivered improved wear resistance and reduced notch and crater wear. The rake face wear that is visible in Figure 10 indicates better abrasion resistance.
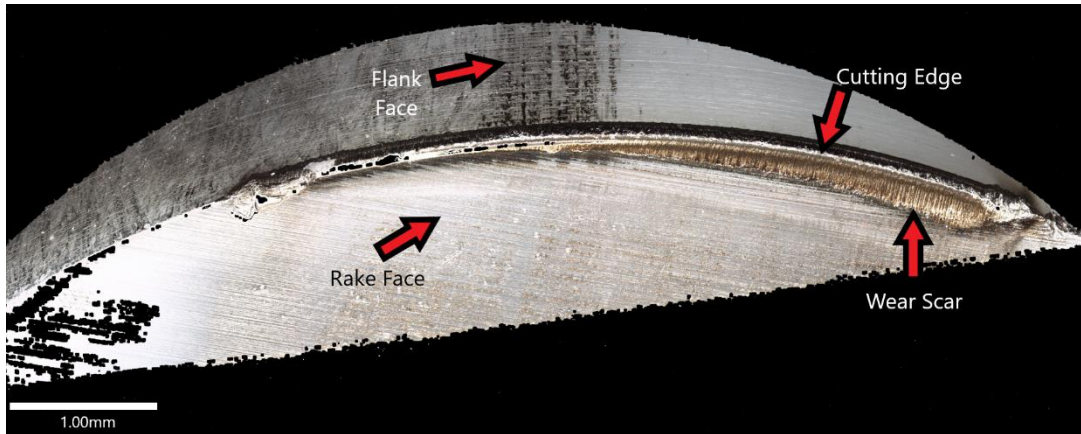
Figure 10. Wear scar on turning insert B (SiAlON grade 1) after test cut 6.2.

The seventh set of test cuts used insert C (SiAlON grade 2), consisting of two cuts at equal length and depth. In Figure 11, a wear scar on turning insert C (SiAlON grade two) after test cut 7.2 is shown.
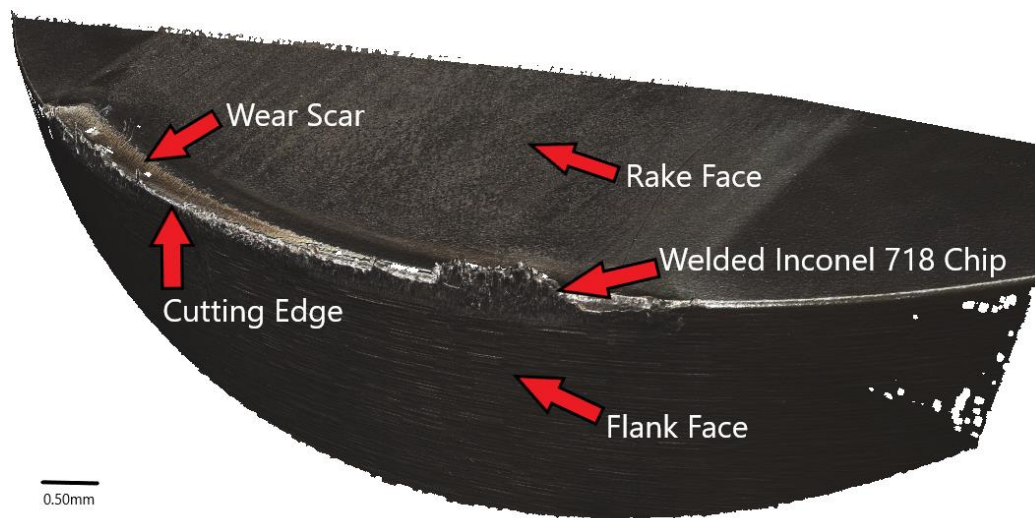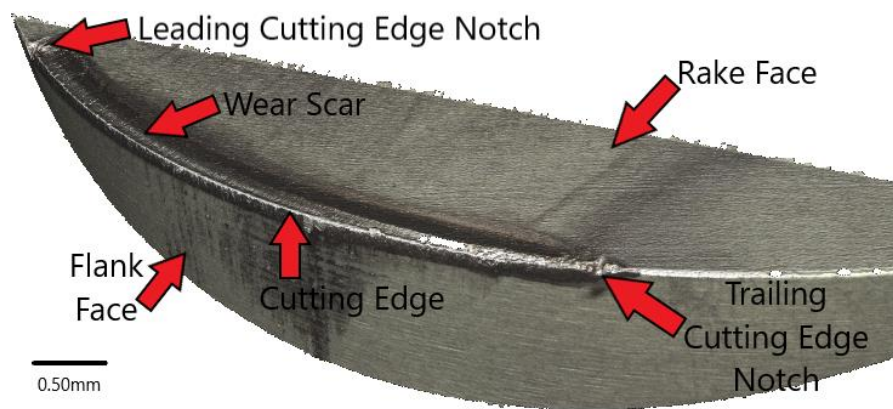

Figure 11. Wear scar on turning insert C (SiAlON grade 2) after test cut 7.2.

The seventh set of test cuts once again provided noticeable improvements in insert wear results when compared to six other sets of test cuts that had taken place beforehand. Insert C showed no real signs of flank wear, crater wear or notch wear. There were slight signs of the abrasion on the rake face but that was to be expected and the lack of wear is visible in Figure 11. The same wear features that can be seen in test cut 5.1 and test cut 6.1, are also evident in test cut 7.1 but considerably less wear was visible. The increase in surface speed has certainly improved the wear resistance of the inserts throughout the second set of tests. It is hypothesised that the reason for the improved resistance to abrasion, flank wear and notching is that tool 5 has a higher hot hardness, lower rates of thermal expansion and thermal conductivity and a tougher microstructure. It is clear that the tougher microstructure

will come from the inclusion of more β-SiAlON grains, and the abrasion resistance and hot hardness will come from the α-SiAlON. The α-SiAlON and β- SiAlONs in tool 5 look to have been hot-pressed to form an insert with superior hot hardness, toughness and abrasion resistance when compared to insert A and insert B.

The eighth set of test cuts utilised insert D (whisker-reinforced alumina grade). The test consisted of two cuts at equal length and depth. Figure 12 shows a wear scar on turning insert D (whisker-reinforced alumina grade) after test cut 8.2. During the eighth set of test cuts, very few vibrations were encountered.

Figure 12. Wear scar on turning insert D (whisker-reinforced alumina grade) after test cut 8.2.

The eighth set of test cuts provided noticeable results when compared to test cuts 5.1-5.2 and 6.1-6.2. Insert D showed no real signs of flank wear, crater wear or notch wear. The cutting edge was in very good shape after test cut 8.1. There were slight signs of the abrasion on the rake face, but that was to be expected considering the cutting conditions. The lack of wear is visible in Figure 12, likely due to the mechanical properties of whisker-reinforced alumina microstructure. The results indicate that tool 6 has a higher modulus and fracture toughness when compared to insert C (SiAlON grade 1, (insert A and B). Insert D is also standard whisker-reinforced alumina grade for hard turning nickel-based alloys and has also delivered results as expected. Insert C (SiAlON grade 2) has attained the least amount of flank wear and this is shown in Figure 13. Insert C and insert D generated similar small wear scars when subjected to the same cutting conditions as the other test cuts. All of the cutting tools experienced considerably less vibration when the cutting speed was increased to 300m/min.
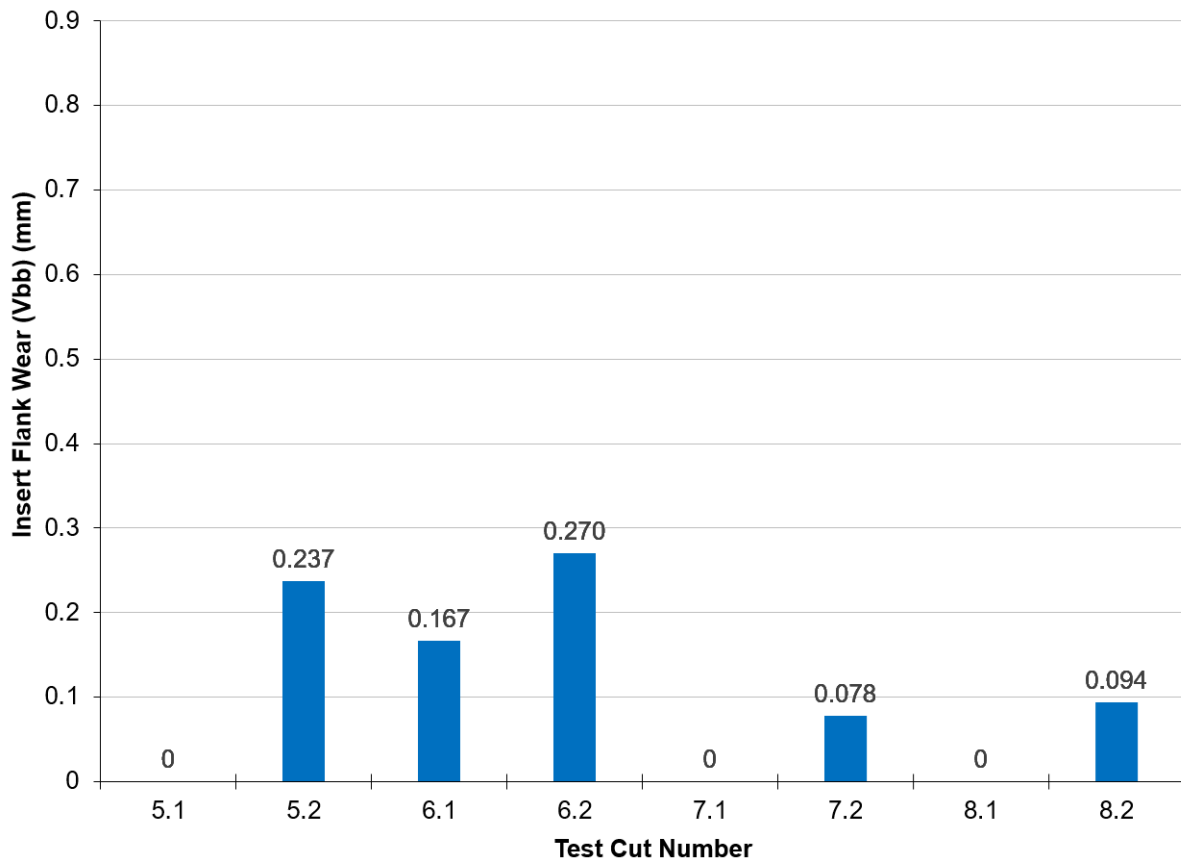
Figure 13. Measured flank wear (Vbb) experienced for each test cut at a cutting speed of 300m/min.

Test cuts 3.1-3.2 (Insert C) and test cuts 7.1-7.2 (Insert C) showed the lowest insert wear when compared to the other test cuts. Tool 5 ultimately outperformed Insert A, B and D in this regard. Each test cut was repeated twice so that correct amount of material was removed. Figure 13 represents raw data directly gathered from the machining trial, so no error bars have been included in the graph.

3.3   Chip analysis

The scanning electron microscope (SEM) image analysis resulted in three images being captured for each of the four swarf chip samples. An SEM image at 500x resolution, 1000x resolution and 2500x resolution was taken. The images captured on FEI F50 SEM highlighted the chip morphology and visually showed the level of deformation that the chip underwent as a result of the machining process. The images for each sample show in detail the brittle failure zones; the highly deformed microstructure of the chip visually highlighted the segmented chip morphology which was a result of fluctuation in specific shear forces during the machining process. The deformation characteristics of Inconel 718 chips followed slip lines and the Burgers vectors of dislocations that are apparent in a face centre cubic crystal structure, these are shown in a Thompson tetrahedron [21].

3.3.1 SEM Sample 1 - Test Cut 4.2

Sample 1 chips were produced with insert D (whisker-reinforced alumina grade) at 250m/min, 0.20 mm/rev, 2mm depth of cut. Figures 14A-B show SEM images demonstrating the common chip morphology characteristics of machining Inconel 718 at a cutting speed of 250m/min. During the machining process, the Inconel material deformed along localised shear planes and formed segments.
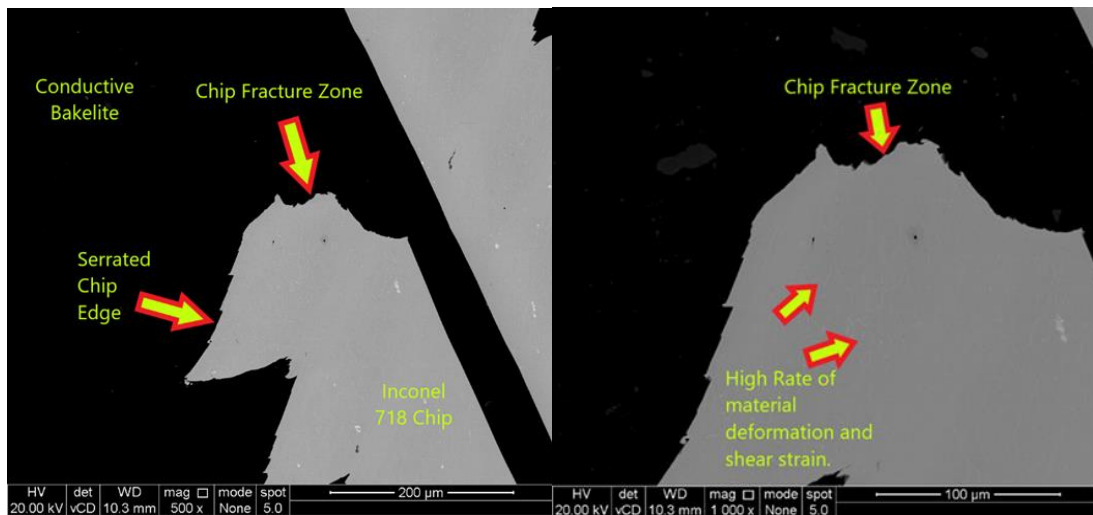

Figure 14. Test Cut 4.2 SEM Image magnified 500x (A), 1000x (B).

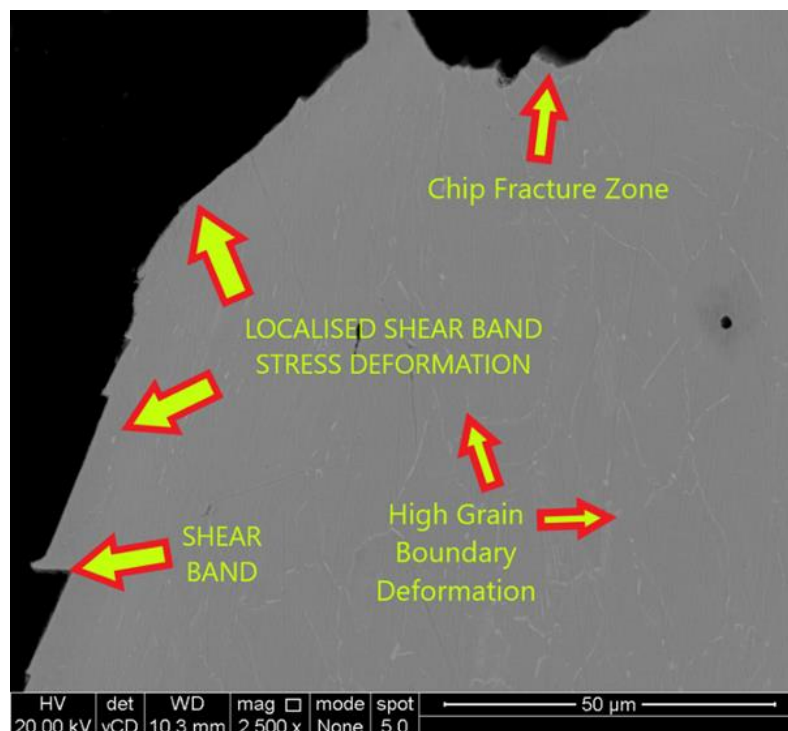High grain boundary deformation or 'twinning' is evident in Figures 14B and 15.

Figure 15. Test Cut 4.2 SEM Image magnified 2500x.

The face centre cubic structure and high strength of Inconel 718 encourage twinning to take place along the (111) planes and in the direction of the (112) plane and this takes place when the material is subjected to a stress state which is below the shear stress state that causes slip systems. If the stress state inverts, then it will follow the (110) plane direction instead of the (111) plane direction. The localised deformation that can be viewed in Figure 16 has also be attained by a study that was conducted by R. Komandur et al [20].

3.3.2 SEM Sample 2 - Test Cut 3.1

Sample 2 chips were produced with an insert C (SiAlON grade 2) at 250m/min, 0.20 mm/rev, 2mm depth of cut). Figures 16A-B show SEM images which visually display the common chip morphology characteristics of machining Inconel 718 at a cutting speed of 250m/min. Figure 16A shows visually the localised shear bands that are generated during the machining process and resulting shear band fracture of the swarf chip. The Inconel 718 chips are characterised to have relatively low deformation in the main section of the segments and evenly positioned localised intense, shear bands between each of the segments. Twinning is evident. The grain boundaries shown in Figure 16B show localised shear band deformation; the shear band deformation caused the Inconel 718 chip to strain harden to the point of fracture.
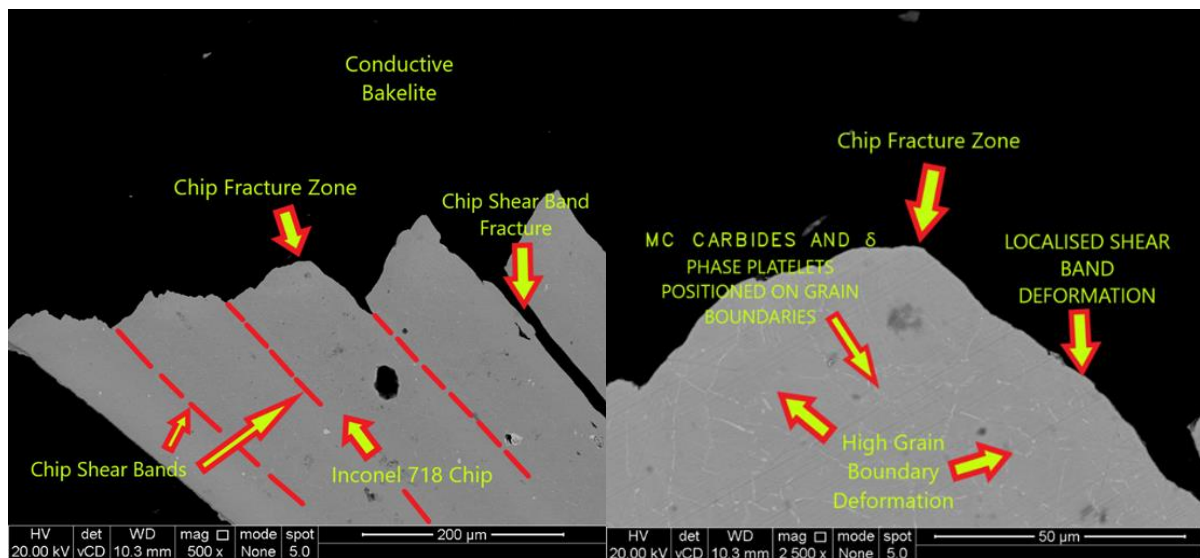

Figure 16. Test Cut 3.1 SEM image magnified 500x (A), 2500x (B).

Figure 16B shows the isolated metal carbides (MC) and the austenite matrix with δ-phase platelets distributed on the grain boundaries. The δ-phase consisted of orthorhombic Ni_3Nb phase, which distributed onto the grain boundaries. The distribution of the metal carbides (MC) and δ-phase on the grain boundaries was due to the very high plastic deformation and cutting temperatures that took place in and around the localised shear band location.

17

3.3.3 SEM Sample 3 - Test Cut 8.1

Sample 3 chips were produced with an insert D (whisker-reinforced alumina grade) at 300m/min, 0.20 mm/rev, and 2mm depth of cut. Figures 17A-B show SEM images which demonstrate the common chip morphology characteristics of machining Inconel 718 at a cutting speed of 300m/min. Figure 17A-B shows visually the localised shear bands that were generated during the machining process. The localised shear stress resulted in a shear band fracture of the chip, which is evident in Figures 17A-B. The increase in cutting speed from 250m/min to 300m/min intensified the localisation of the critical shear stress into localised bands. The cutting temperatures of the primary shear zone also rose with an increase in the cutting speed. Similar results were gathered by Z. P. Hao et al.[18] . In their study of characterising shear band localisation in Inconel 718 that had been machined at high cutting speeds.
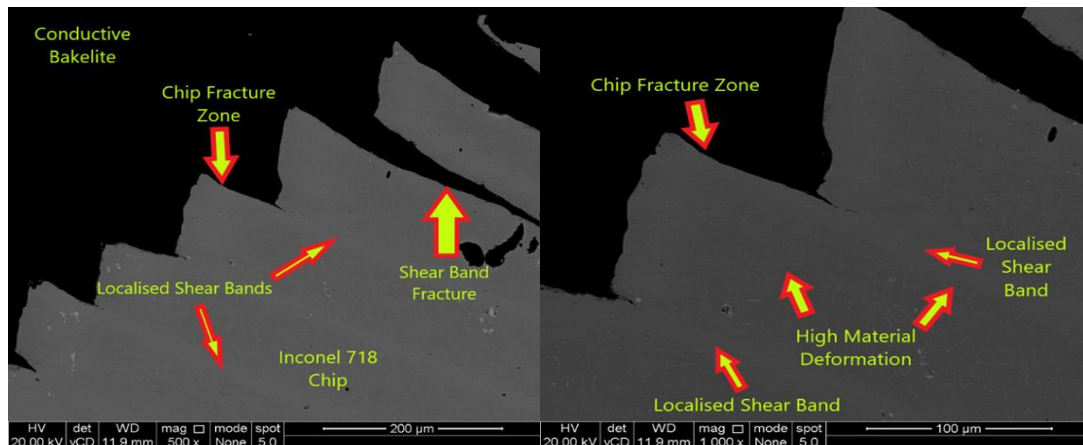

Figure 17. Test Cut 8.1 SEM image magnified 500x (A), 1000x (B).

3.3.4 SEM Sample 4 - Test Cut 7.2

Sample 2 chips were produced with an insert C (SiAlON grade 2) at 300m/min, 0.20 mm/rev, 2mm depth of cut. Figures 18A-B show SEM images displaying the common chip morphology characteristics of machining Inconel 718 at a cutting speed of 300m/min. Figure 19 shows the isolated MC carbides and the austenite matrix with δ-phase platelets distributed on the grain boundaries.
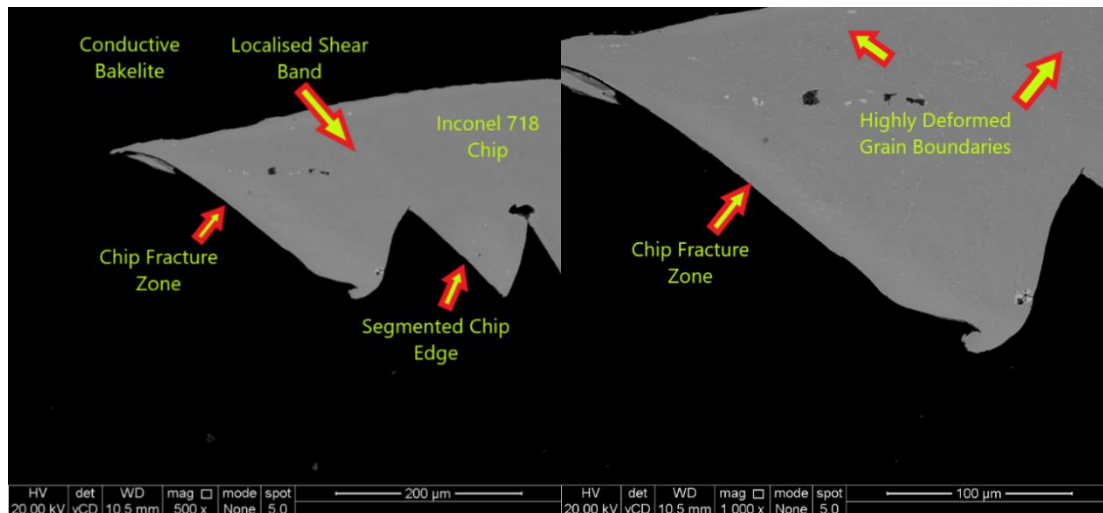
Figure 18. Test Cut 7.2 SEM image magnified 500x (A), 1000x (B).

Plastic deformation consolidated at the outer edges of the chip due to strain hardening. The bulk of the chip was not as deformed as the highly deformed localised regions near the chip fracture zone. The types of serrated chip morphology which can be viewed in Figures 18A-B and 19, are also highly evident in the study which was conducted by Zhang [17], that study was particularly focused on the evaluation of the fluctuation of cutting forces when turning Inconel 718.
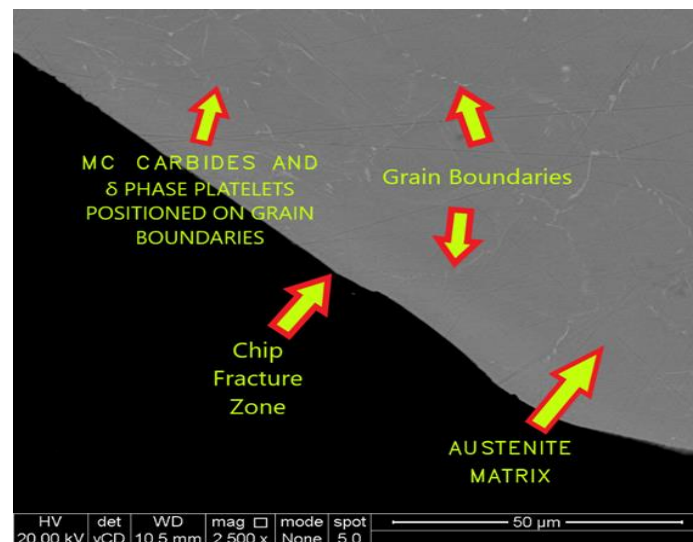

Figure 19. Test Cut 7.2 SEM image magnified 2500x.

4 Discussion

4.1 Insert Wear Analysis

During the machining trial, one of the prominent factors that was of interest was the amount of vibration which was encountered by each test cut. In test cut 1.1, large vibrations were experienced by the machine and the cutting tool. Figure 4 shows the end result of these

vibrations and Figure 3 shows how these large vibrations have had a catastrophic effect on the life of the tool. The reasons for the high vibrations could be due to the failure of the cutting tool edge for test 1.1 (Insert A). The roll in to cut will have generated an initial shock which caused a large crater to form on the cutting tool edge. This is interesting because the same roll in to cut approach was utilised throughout the machining trial. Notch wear is also visible, and the first cut generated a large amount of flank wear. The decision to fail the insert was taken due to it surpassing the default value of 1mm for a wear scar.

Test cut 2.1 also encountered some vibration over the first 25 mm of the cut and then stopped and cleaned up to provide a good surface finish. The flank wear in test cut 2.2 was still pretty high when compared to the other test cuts and the wear scars for test cut 2.2 were measured to be just under the default failure value. Test cut 3.1 and 3.2 adopted the same 0.20mm/rev feed rate and 2mm depth of cut but the surface finish was a lot better than the first two sets of test cuts when conducted at a 250m/min surface speed. Test cut 3.1 and test 3.2 delivered impressive abrasion resistance results when compared to the first two test cuts.

Test Cut 4.1 also delivered notable abrasion resistance when subjected to the same cutting conditions. There was very little vibration encountered in test cut 4.1- 4.2 (Insert D), the reduction of vibration contributed to a subsequent reduction in overall wear that the insert sustained and this visible in Figures 7 and 12. Insert D showed high stability and high resistance to notching and resistance to flank wear.

Test cuts 5.1-5.2 (Tool 3), 6.1-6.2 (Tool 4), 7.1-7.2 (Insert C) and 8.1-8.2 (Insert D) all managed to attain substantially better wear resistance results when compared to test 1.1 (Insert A), Test cuts 2.1-2.2 (Insert B), 3.1-3.2 (Insert C) and 4.1-4.2 (Insert D). The increase in cutting speed from 250m/min to 300m/min seemed to improve the wear resistance capability of the inserts in the second set of test cuts. The improvements in wear resistance can be attributed to the higher cutting temperatures being created in the tool-chip interface as a result of the increase in cutting speed; this in turn reduced the perspective yield strength of the Inconel 718 material and the necessary cutting forces. The variation in chip morphology is a result of the fluctuations in cyclic specific shear forces being higher than that of continuous cutting forces, and it is this that causes the serrated chip morphology. The serrated chip effect is a result of shear bands forming between each of the serrated edges. The width of the shear band should decrease as the cutting speed is increased. The shear bands of the chip can be more clearly inspected on a scanning electron microscope.

Throughout the machine trial, the finish cut diameter was measured to see what level of accuracy was achieved with each cut. Some work-piece spring-back was observed in the

material in the FY axis and also some loss of rigidity in the machine. The required material removal was never exactly 273cm^3, but apart from the failure test cut 1.1, all of the test cuts were deemed to be a success.

4.2   Chip Morphology Analysis

During the study of the chip morphology and the stain hardening of the Inconel 718 chip, the focus was to gain an understanding of what happens to the swarf chip at different cutting speeds. The high cutting speeds that were used to create the Bakelite samples yielded shear localised chips. In each of the samples, a segmented and serrated edge chip profile typical of high-speed turning was evident. There were two stages involved in the chip formation process at these types of speeds. One stage comprised plastic instability and the other stage involved strain localisation in a narrow band in the primary shear zone. Samples one and two showed clear signs of localised deformation in and around the chip fracture zones due to twinning and localised shear.

The other stages which were involved in the formation of the Inconel 718 chip at high cutting speeds involved the formation of segments as the cutting tool advanced. Sample two seemed to show slightly higher shear localisation when compared to samples one - this was due to the increase in cutting speed. During the latter stage, the chip experienced significant amounts of shear. The high cutting speed caused the chip to deform locally; the deformation in the localised shear bands ultimately causing the chip material to strain harden to the point of fracture. As the cutting speed increased, the length of contact between the segments decreased, which increased the shear strain, evident in Figure 2D, which showed feathered chip segments were the result of reduced amounts of contact. The increase in periodic segmentation was due to the increase in cutting speed and this was evident in sample three, in Figure 17A.

The discontinuous chips that were produced at cutting speeds of 250m/min and 300m/min all ultimately led to chip fracture due to strain localisation in the primary shear zone. The primary shear zone was exposed to higher cutting temperatures when the cutting speed increased from 250m/min to 300m/min. With the increase in cutting speeds, the cutting forces reduced because of the higher shear zone temperatures, reducing the yield strength of the Inconel 718 material. The cutting conditions that were experienced at the two cutting speeds by the chip and the cutting tool were extreme. The poor thermal conductivity properties of Inconel 718 concentrated the heat into narrow deformation shear bands, which generate highly deformed localised chip segments. This created an extreme machining environment. The extreme cutting conditions caused the simultaneous fluctuation between the stress and strain in the Inconel 718 material. The extreme cutting environment ultimately

yielded the shear localised chip in all four of the Bakelite samples used in this study. When machining hard to machine materials such as Inconel 718, it is important to utilise the correct machining parameters such as cutting speed, feed rate and depth of cut as these parameters have a noticeable effect on the amount tool wear that is generated, and ultimately, the tool life. When using ceramic cutting tools, a compromise needs to be made so that the tool life is optimum with the serrated type of the swarf chip that is being produced. The surface finish of the Inconel 718 after the second cut with all four different ceramic turning inserts was very good and shows that a cutting speed of 300m/min and feed rate of 0.2mm/rev can attain a such a finish. This cutting speed will result in an increase in intense shear band localization within the chip, however, this is just a by-product of the increase in cutting speed. The use of a 300m/min cutting speed and 0.2mm/rev feed rate will result in higher productivity and will allow for a good surface finish. These cutting conditions have been typically advised by industrial cutting tool suppliers for a number of years, but the level of wear seen during this machining trial is an improvement on what has been achieved in previous research studies [5] & [19].

5 Conclusions

The conclusions from chip morphology drawn from the turning of Inconel 718 with silicon nitride Si_3N_4 based ceramic and whisker-reinforced alumina ($Al_2O_3 + Si\ C_w$) inserts are as follows:

1. Several wear mechanisms (flank, crater, notching, and plastic deformation) can occur and specifically when using round inserts, flank and notch wear are dominant. Notch wear was the most predominant wear mechanism that was captured during this machining trial.

2. The optimum cutting speed for machining Inconel 718 is 300 m/min. At cutting speeds above 250m/min, intense shear band localisation in the primary shear zone of the chip/tool interface leads to increasing levels of chip segmentation and failure.

3. It is recommended that a SiAlON grade 2 round cutting tool insert is used for rough machining of Inconel 718.

Acknowledgements

References

[1]   V. Ramaswamy, P. R. Swann, and D. R. F. West, "Observation on Intermetallic Compound and Carbide Precipitation in Two Commercial Nickel-based Superalloys," *J. Less Common Metals t.* vol. 27, 1972.

[2]   R. Y. Zhang *et al.*, "Evolution of Lattice Spacing of Gamma Double Prime Precipitates During Aging of Polycrystalline Ni-Base Superalloys : An In Situ Investigation," *Metall. Mater. Trans. A*, vol. 51A, 2019.

[3]   B. Wang and Z. Liu, "Influences of tool structure, tool material and tool wear on machined surface integrity during turning and milling of titanium and nickel alloys: a review," *Int. J. Adv. Manuf. Technol.*, vol. 98, no. 5–8, pp. 1925–1975, 2018.

[4]   K. Zhuang, D. Zhu, X. Zhang, and H. Ding, "Notch wear prediction model in turning of Inconel 718 with ceramic tools considering the influence of work hardened layer," *Wear*, vol. 313, no. 1–2, pp. 63–74, 2014.

[5]   A. Altin, M. Nalbant, and A. Taskesen, "The effects of cutting speed on tool wear and tool life when machining Inconel 718 with ceramic tools," *Mater. Des.*, vol. 28, no. 9, pp. 2518–2522, 2007.

[6]   I. . Choudhury and M. . El-Baradie, "Machinability of nickel-base super alloys: a general review," *J. Mater. Process. Technol.*, vol. 77, no. 1–3, pp. 278–284, 1998.

[7]   E. O. Ezugwu, J. Bonney, and Y. Yamane, "An overview of the machinability of aeroengine alloys," *J. Mater. Process. Technol.*, vol. 134, no. 2, pp. 233–253, 2003.

[8]   M. A. Shalaby and S. C. Veldhuis, "Wear and Tribological Performance of Different Ceramic Tools in Dry High Speed Machining of Ni-Co-Cr Precipitation Hardenable Aerospace Superalloy," *Tribol. Trans.*, vol. 0, no. 0, pp. 1–40, 2018.

[9]   A. Suarez, L. N. López de Lacalle, R. Polvorosa, F. Veiga, A. Wretland, " Effects of high-pressure cooling on the wear patterns on turning inserts used on alloy IN718," J Mat & Manuf Processes., vol. 32, no. 6, 678–686, 2017.

[10]   Z. Vagnorius and K. Sørby, "Effect of high-pressure cooling on life of SiAlON tools in machining of Inconel 718," Int J Adv Manuf Technol, vol 54 pp. 83–92, 2011.

[11]   R. Polvorosa, A. Suárez, L. N. L. de Lacalle, I. Cerrillo, A. Wretland, and F. Veiga, "Tool wear on nickel alloys with different coolant pressures: Comparison of Alloy 718 and Waspaloy," *J. Manuf. Process.*, vol. 26, pp. 44–56, 2017.

23

[12] E. O. Ezugwu and J. Bonney, "Effect of high-pressure coolant supply when machining nickel-base, Inconel 718, alloy with coated carbide tools," *J. Mater. Process. Technol.*, vol. 153–154, no. 1–3, pp. 1045–1050, 2004.

[13] W. H. Pereira and S. Delijaicow, "Surface intergrity of Inconel 718 turned under cryogenic conditions at high cutting speeds," *Int. J. Adv. Manuf. Technol.*, vol. 104, pp. 2163-2177, 2019.

[14] V, Sivalingam, Z, Zan, J, Sun, "Wear behaviour of whicker-reinforced ceramic tools in the turning of Inconel 718 assisted by an atomized spray of solid lubricants,"J.Tribo Int., vol. 148, pp.106-235, 2020.

[15] A. Marques, M. P. Suarez, W. F. Sales, Á. R. Machado, "Turning of Inconel 718 with whisker-reinforced ceramic tools applying vegetable -based cuttng fluid mixed with solid lubricants by MQL," J. Mat. Process. Tech., vol. 266, pp.530–543, 2019.

[16] N. S. Bhadoria, G. Bartarya, " On the improvement in process performance of ceramic inserts during hard turning in MQL environment." J. Mat & Manuf. Process., 2021. https://doi.org/10.1080/10426914.2021.1967978.

[17] S. Zhang, J. Li, X. Zhu, and H. Lv, "Saw-tooth chip formation and its effect on cutting force fluctuation in turning of Inconel 718," *Int. J. Precis. Eng. Manuf.*, vol. 14, no. 6, pp. 957–963, 2013.

[18] Z. P. Hao, R. R. Cui, and Y. H. Fan, "Formation mechanism and characterisation of shear band in high-speed cutting Inconel718," *Int. J. Adv. Manuf. Technol.*, vol. 98, no. 9–12, pp. 2791–2799, 2018.

[19 R.P.Zeilmann, F.Fontanive, R.M.Soares, "Wear mechanisms during dry and wet turning of Inconel 718 with ceramic tools," Int.J.Adv Manuf Technol.,vol. 92, pp. 2705-2714, 2017.

[20] R. Komandur and T. A. Schroeder, "On shear instability in machining a nickel-iron base superalloy," *J. Manuf. Sci. Eng. Trans. ASME*, vol. 108, no. 2, pp. 93–100, 1986.

[21] S. M. Corporation, "INCONEL alloy 718," 2014.

[22] G. Brandt, A. Gerendas, and M. Mikus, "Wear mechanisms of ceramic cutting tools when machining ferrous and non-ferrous alloys," *J. Eur. Ceram. Soc.*, vol. 6, no. 5, pp. 273–290, 1990.

[23] J. Aucote and S. R. Foster, "Performance of SiAlON cutting tools when machining nickel-base aerospace alloys," *Mater. Sci. Technol.*, vol. 2, no. 7, pp. 700–708, 1986.

[24] Y. T. Zhu, X. L. Wu, X. Z. Liao, J. Narayan, L. J. Kecskés, and S. N. Mathaudhu, "Dislocation-twin interactions in nanocrystalline fcc metals," *Acta Mater.*, vol. 59, no. 2, pp. 812–821, 2011.

1
2
3
4
5
6
7
8
9
10
11
12
13
14
15
16
17
18
19
20
21
22
23
24
25
26
27
28
29
30
31
32
33
34
35
36
37
38
39
40
41
42
43
44
45
46
47
48
49
50
51
52
53
54
55
56
57
58
59
60
61
62
63
64
65